

Urine proteomic analysis of the rat e-cigarette model

Yuqing Liu¹, Ziyun Shen¹, Chenyang Zhao¹, Youhe Gao^{Corresp. 1}

¹ Gene Engineering Drug and Biotechnology Beijing Key Laboratory, Beijing Normal University, Beijing, China

Corresponding Author: Youhe Gao
Email address: gaoyouhe@bnu.edu.cn

Background. We were curious if the urinary proteome could reflect the effects of e-cigarettes on the organism. **Methods.** Urine samples were collected from a rat e-cigarette model before, during, and after two weeks of e-cigarette smoking. Urine proteomes before and after smoking of each rat were compared individually, while the control group was set up to rule out differences caused by rat growth and development. **Results.** Fetuin-B, a biomarker of Chronic obstructive pulmonary disease(COPD), and annexin A2, which is recognized as a multiple tumour marker, were identified as differential proteins in five out of six smoking rats on day 3. To our surprise, odourant-binding proteins expressed in the olfactory epithelium were also found and were significantly upregulated. Pathways enriched by the differential proteins include the apelin signalling pathway, folate biosynthesis pathway, arachidonic acid metabolism, chemical carcinogenesis-DNA adducts and chemical carcinogenesis-reactive oxygen species. They have been reported to be associated with immune system, cardiovascular system, respiratory system, etc. **Conclusions.** Urinary proteome could reflect the effects of e-cigarettes in rats.

Urine proteomic analysis of the rat e-cigarette model

Yuqing Liu¹ Ziyun Shen¹ Chenyang Zhao¹ Youhe Gao^{1,*}

¹Gene Engineering Drug and Biotechnology Beijing Key Laboratory, College of Life Sciences, Beijing Normal University, Beijing 100875, China

Corresponding Author:

Youhe Gao¹

Beijing Normal University, Beijing 100875, China

Email address: *gaoyouhe@bnu.edu.cn

Abstract

Background. We were curious if the urinary proteome could reflect the effects of e-cigarettes on the organism. **Methods.** Urine samples were collected from a rat e-cigarette model before, during, and after two weeks of e-cigarette smoking. Urine proteomes before and after smoking of each rat were compared individually, while the control group was set up to rule out differences caused by rat growth and development. **Results.** Fetuin-B, a biomarker of Chronic obstructive pulmonary disease (COPD), and annexin A2, which is recognized as a multiple tumour marker, were identified as differential proteins in five out of six smoking rats on day 3. To our surprise, odourant-binding proteins expressed in the olfactory epithelium were also found and were significantly upregulated. Pathways enriched by the differential proteins include the apelin signalling pathway, folate biosynthesis pathway, arachidonic acid metabolism, chemical carcinogenesis-DNA adducts and chemical carcinogenesis-reactive oxygen species. They have been reported to be associated with immune system, cardiovascular system, respiratory system, etc. **Conclusions.** Urinary proteome could reflect the effects of e-cigarettes in rats.

Keywords: urine; proteomics; e-cigarette model; odourant-binding protein

Introduction

1.1 E-cigarettes

E-cigarettes are mainly composed of four parts: soot oil, a heating system, a power supply and a filter nozzle. Aerosols with specific odours are generated by heating atomization for smokers. The main components of the aerosol liquid of the electronic vapourizer are plant glycerin, propylene glycol, edible flavour and nicotine salt. As of 2019, approximately 10 million people aged 15 years and older in China had used e-cigarettes^[1]. The population using e-cigarettes is predominantly young adults, with the highest use in the 15- to 24-year age group^[1]. The vast majority (58.3%) of middle school e-cigarette users use fruit-flavoured e-cigarettes, and previous research suggests that these tastes may attract young people to try e-cigarettes^[2]. On May 1, 2022, the *Regulations on the Administration of Electronic Tobacco* prohibited the use of electronic cigarettes with flavours other than tobacco tastes. Pipe AL et al.^[3] found that the composition of heated chemical aerosols inhaled by the human body after electron fumigation is

42 very complex and includes nicotine, nitrosamines, carbonyl compounds, heavy metals, free
43 radicals, reactive oxygen species, particulate matter, and “emerging chemicals of concern”,
44 which further demonstrates the potential harm of smoking e-cigarettes. Studies have shown that
45 smoking e-cigarettes may increase the risk of lung disease^[4] and cardiovascular disease^{[5]-[6]} and
46 may cause harm to the liver^[7], urinary system^[8], and immune system^[9]. In pregnant women,
47 exposure to e-cigarettes causes harm to the mother and the foetus. Ballbè M et al.^[10] detected low
48 but nonnegligible concentrations of e-smoke-associated analytes in cord blood and breast milk of
49 nonuser pregnant women exposed to e-cigarettes. Aslaner DM et al.^[11] also demonstrated that
50 the inhalation of secondhand e-cigarette smoke by pregnant women can have long-term effects
51 on the lungs of offspring. At the same time, because the nicotine content in e-cigarette smoke is
52 equivalent to or even higher than that in combustible smoke^[12], the damage caused by e-cigarette
53 smoke to the human body cannot be ignored.

54 **1.2 Urine biomarkers**

55 Biomarkers are indicators that can objectively reflect normal pathological processes as well
56 as physiological processes^[13], and clinically, biomarkers can predict, monitor, and diagnose
57 multifactorial diseases at different stages^[14]. The potential of urinary biomarkers has not been
58 fully explored compared to the more widely used blood biomarkers, especially in terms of early
59 diagnosis of disease and status prediction. Because the homeostatic mechanisms are regulated in
60 the blood, changes in the blood proteome caused by a particular disease are metabolically
61 excreted, and no significant changes are apparent in the early stages of a disease. In contrast, as a
62 filtrate of the blood, urine bears no need or mechanism for stability; thus, minor changes in the
63 disease at an early stage can be observed in urine^[15], which indicates that urine is a good source
64 of biomarkers.

65 Currently, the detection of biomarkers in urine has attracted increasing attention from
66 clinicians and researchers. This approach has been used in the treatment and research of a variety
67 of diseases, such as pulmonary fibrosis^[16], colitis^[17], glioma^[18] and other diseases. Studies have
68 shown that urine biomarkers can classify diseases, such as predicting chronic kidney disease
69 (CKD)^[19] and distinguishing benign and malignant ovarian cancer^[20]. Urine biomarkers can also
70 be used to detect whether complete resection and recurrence occur after tumour surgery so that
71 adjustments can be made in time to reduce the risk of recurrence. Pharmacologically, urinary
72 biomarkers may indicate the utility of drugs in the body, such as predicting the efficacy of
73 rituximab therapy in adult patients with systemic lupus erythematosus (SLE) and determining
74 that sacubitril-valsartan is more effective than valsartan in the treatment of chronic heart
75 failure^[21]. In terms of exercise physiology, urine biomarkers can reflect changes in urine
76 proteomics after exercise, thus providing a scientific basis for the rational training of athletes^[22].
77 In recent years, many studies have shown that urine proteomics can also reveal biomarkers in
78 neurodegenerative diseases and psychiatric diseases, such as Parkinson’s disease^[23]-Error! Reference
79 source not found., Alzheimer’s disease^[25], depression^[26], autism^[27] and other diseases.

80 However, there have been no studies on e-cigarettes in the field of urine proteomics. The
81 urine proteome is susceptible to multiple factors, such as diet, drug therapy, and daily activities.
82 To make the experimental results more accurate, it is critical to use a simple and controllable
83 system. Because the genetic and environmental factors associated with animal models can be
84 artificially controlled and the influence of unrelated factors can be minimized, the use of animal
85 models is a very appropriate experimental method. Therefore, we constructed an animal model to
86 analyse the urine proteomics of the rat e-cigarette model, and the experimental workflow is
87 shown in Fig 1. We aimed to determine the effect of smoking e-cigarettes on the urine proteome

88 of rats.

89

90

91 **2 Materials and Methods**

92 **2.1 Rat model establishment**

93 Portions of this text were previously published as part of a preprint^[28]. Eleven SPF (specific
94 pathogen free) 8-week-old healthy male Wistar rats (180-200 g) were purchased from Beijing
95 Vital River Laboratory Animal Technology Co., Ltd., with the animal licence number SYXK
96 (Jing) 2021-0011. All rats were maintained in a standard environment (room temperature
97 $(22\pm 1)^{\circ}\text{C}$, humidity 65%–70%). The environmental equipment for animal experiments met the
98 requirements of the standards for experimental animal grades, and qualified feed, cages, bedding
99 and other supplies were used. All rats were kept in a new environment for three days before
100 starting the experiment. At the end of the experiment, the rats were euthanized according to the
101 standard. Our method of euthanasia was cervical dislocation following anaesthesia. Anaesthesia
102 was induced with 0.41 mL of 2% isoflurane per minute. All experimental procedures were
103 reviewed and approved by the Ethics Committee of the College of Life Sciences, Beijing Normal
104 University (Approval No. CLS-AWEC-B-2022-003). All experimental procedures were carried
105 out and reported in compliance with the ARRIVE guidelines.

106 The animal model of e-cigarette use was established by randomly dividing 11 rats into an
107 experimental group and a control group. Five of the control rats were maintained in a standard
108 environment for 17 days. Six rats in the experimental group smoked e-cigarettes once a day
109 during the same period. We used a syringe to simulate the process of inhaling e-cigarette smoke
110 from a human mouth and injected the resulting smoke into the rat cages. One-third of the 3%
111 nicotine e-cigarette refill cartridges was made into smoke (approximately 16 mg of nicotine) and
112 evenly injected into two cages [36 cm (length) \times 20 cm (width) \times 28 cm (height)]. Under the
113 condition of ensuring adequate oxygen content, three rats in the experimental group were placed
114 in each cage and continued to smoke for 1 h for 14 days. They were returned to their original
115 cages after each smoking treatment. Rats were observed for behavioural changes during the
116 experiment, and body weights were recorded every 5 days.

117 **2.2 Urine collection**

118 After all rats were kept in a new environment for three days, they were uniformly placed in
119 metabolic cages to collect urine samples for 12 h. Urine samples were collected during a 12-h
120 period in metabolic cages (DXL-D, made by Beijing Jiayuan Xingye Technology Co., Ltd.) from
121 all rats on days 3, 6, 9, and 12 of e-cigarette smoking and on days 1 (equivalent to day 15) and 3
122 (equivalent to day 17) of cessation of e-cigarette smoking. Rats were fasted and water-deprived
123 during urine collection, and all collected urine samples were stored in a -80°C freezer.

124 **2.3 Treatment of the urine samples**

125 We wanted to observe the sensitivity of the urine proteome and to observe whether the
126 changes within the rat body could be reflected in the urine proteome after smoking e-cigarettes
127 for a short time. Therefore, five time points, namely, nonsmoking day 0, smoking days 3 and 12,
128 and smoking cessation days 1 and 3, were selected as the samples for this focused analysis.

129 Urine protein extraction and quantification: Rat urine samples collected at five time points
130 were centrifuged at $12,000\times g$ for 40 min at 4°C , and the supernatants were transferred to new
131 Eppendorf (EP) tubes. Three volumes of precooled absolute ethanol was added, and the samples
132 were homogeneously mixed and precipitated overnight at -20°C . The following day, the mixture

133 was centrifuged at 12,000×g for 30 min at 4 °C, and the supernatant was discarded. The protein
134 pellet was resuspended in lysis solution (containing 8 mol/L urea, 2 mol/L thiourea, 25 mmol/L
135 dithiothreitol, and 50 mmol/L Tris). The samples were centrifuged at 12,000×g for 30 min at 4
136 °C, and the supernatant was placed in a new EP tube. The protein concentration was measured by
137 the Bradford assay.

138 Urine proteins were digested with trypsin (Trypsin Gold, Mass Spec Grade, Promega,
139 Fitchburg, Wisconsin, USA) using FASP methods^[29]. Urinary protease cleavage: A 100-µg urine
140 protein sample was added to the filter membrane (Pall, Port Washington, NY, USA) of a 10-kDa
141 ultrafiltration tube and placed in an EP tube, and 25 mmol/L NH₄HCO₃ solution was added to
142 make a total volume of 200 µL. Then, 20 mM dithiothreitol solution (dithiothreitol, DTT, Sigma)
143 was added, and after vortex mixing, the metal bath was heated at 97 °C for 5 min and cooled to
144 room temperature. Iodoacetamide (Iodoacetamide, IAA, Sigma) was added at 50 mM, mixed
145 well and allowed to react for 40 min at room temperature in the dark. Then, the following steps
146 were performed: ① membrane washing – 200 µL of UA solution (8 mol/L urea, 0.1 mol/L Tris-
147 HCl, pH 8.5) was added and centrifuged twice at 14,000×g for 5 min at 18 °C; ② Loading –
148 freshly treated samples were added and centrifuged at 14,000×g for 40 min at 18 °C; ③ 200 µL
149 of UA solution was added and centrifuged at 14,000×g for 40 min at 18 °C, repeated twice; ④
150 25 mmol/L NH₄HCO₃ solution was added and centrifuged at 14,000×g for 40 min at 18 °C,
151 repeated twice; and ⑤ trypsin (Trypsin Gold, Promega, Trypchgburg, WI, USA) was added at a
152 ratio of 1:50 trypsin:protein for digestion and kept in a water bath overnight at 37 °C. The
153 following day, peptides were collected by centrifugation at 13,000×g for 30 min at 4 °C, desalted
154 through an HLB column (Waters, Milford, MA), dried using a vacuum dryer, and stored at -80
155 °C.

156 2.4 LC–MS/MS analysis

157 The digested samples were reconstituted with 0.1% formic acid, and peptides were
158 quantified using a BCA kit, followed by diluting of the peptide concentration to 0.5 µg/µL.
159 Mixed peptide samples were prepared from 4 µL of each sample and separated using a high pH
160 reversed-phase peptide separation kit (Thermo Fisher Scientific) according to the instructions.
161 Ten effluents (fractions) were collected by centrifugation, dried using a vacuum dryer and
162 reconstituted with 0.1% formic acid. iRT reagent (Biognosys, Switzerland) was added at a
163 volume ratio of sample:iRT of 10:1 to calibrate the retention times of extracted peptide peaks.
164 For analysis, 1 µg of each peptide from an individual sample was loaded onto a trap column and
165 separated on a reverse-phase C18 column (50 µm×150 mm, 2 µm) using the EASY-nLC1200
166 HPLC system (Thermo Fisher Scientific, Waltham, MA)^[30]. The elution for the analytical
167 column lasted 120 min with a gradient of 5%–28% buffer B (0.1% formic acid in 80%
168 acetonitrile; flow rate 0.3 µL/min). Peptides were analysed with an Orbitrap Fusion Lumos
169 Tribrid Mass Spectrometer (Thermo Fisher Scientific, MA).

170 To generate the spectrum library, 10 isolated fractions were subjected to mass spectrometry
171 in data-dependent acquisition (DDA) mode. Mass spectrometry data were collected in high
172 sensitivity mode. A complete mass spectrometric scan was obtained in the 350–1500 m/z range
173 with a resolution set at 60,000. Individual samples were analysed using Data Independent
174 Acquisition (DIA) mode. DIA acquisition was performed using a DIA method with 36 windows.
175 After every 10 samples, a single DIA analysis of the pooled peptides was performed as a quality
176 control.

177 2.5 Database searching and label-free quantitation

178 Data were collected as previously described by Weijing (2019)^[31]. Specifically, raw data

179 collected from liquid chromatography–mass spectrometry were imported into Proteome
180 Discoverer (version 2.1, Thermo Scientific) and the Swiss-Prot rat database (published in May
181 2019, containing 8086 sequences) for alignment, and iRT sequences were added to the rat
182 database. Then, the search results were imported into Spectronaut Pulsar (Biognosys AG,
183 Switzerland) for processing and analysis. Peptide abundances were calculated by summing the
184 peak areas of the respective fragment ions in MS₂. Protein intensities were summed from their
185 respective peptide abundances to calculate protein abundances.

186 **2.6 Statistical analysis**

187 Two technical replicates were performed for each sample, and the average was used for
188 statistical analysis. In this experiment, the experimental group samples at different time periods
189 were compared before and after, and the control group was set up to rule out differences in
190 growth and development. The identified proteins were compared to screen for differential
191 proteins. The differential protein screening conditions were as follows: fold change (FC) ≥ 1.5 or
192 ≤ 0.67 between groups and P value < 0.05 by two-tailed unpaired t test analysis. The Wu Kong
193 platform was used for the selected differential proteins
194 (<https://www.omicsolution.com/wkomics/main/>); the UniProt website (Release 2023_01)
195 (<https://www.uniprot.org/>) and the DAVID database^[32] (December 22, 2022, DAVID
196 Knowledgebase v2022q4 released) (<https://david.ncifcrf.gov/>) were used to perform functional
197 enrichment analysis. In the PubMed database (<https://pubmed.ncbi.nlm.nih.gov/>), the reported
198 literature was searched to perform functional analysis of differential proteins.

199

200 **3 Results**

201 **3.1 Characterization of e-cigarette smoking rats**

202 In this experiment, the rats were observed behaviourally during the modelling process.
203 Among them, rats in the control group had normal activity and normal dietary and drinking water
204 intake. Water intake was significantly increased in the treated group compared with the control
205 group. At the same time, the body weight of the rats was recorded every 5 days in this
206 experiment (Fig 2), and a significant increase in individualized variance in the body weight of
207 the rats in the experimental group was observed.

208 **3.2 Urinary proteome changes**

209 **3.2.1 Urine protein identification**

210 Fifty-five urine protein samples were analysed by LC–MS/MS tandem mass spectrometry
211 after the rat e-cigarette model was established. In total, 1093 proteins were identified (≥ 2
212 specific peptides and FDR $< 1\%$ at the protein level).

213 **3.2.2 Urine proteome changes**

214 With the aim of investigating whether the changes were consistent in the six treated rats, we
215 performed urine proteomics analysis of each rat individually as its own control and compared
216 them at different time points to D0 (Fig 3). The screening differential protein conditions were FC
217 ≥ 1.5 or ≤ 0.67 and two-tailed unpaired t test $P < 0.05$. The differential protein screening results
218 are shown in Table 1.

219 To observe the consistency of the changes in the six treated rats more intuitively, we made
220 Venn diagrams of the differential proteins screened by comparing the six rats in the experimental
221 group before (D0) and after on D3, D12, D15, and D17 (Fig 4).

222 To verify the correlation between rat differential proteins at different time points, we made
223 Venn diagrams. These diagrams show the common differential proteins identified in urine

224 protein from five or more treated rats on D3, D12, D15, and D17 compared with D0 (Fig 5).
225 Among them, cadherin was screened by 5 or more rats at all four time points, and all showed a
226 tendency towards downregulation. Six differential proteins were screened by 5 or more rats at all
227 three time points, showing more common differences. The trends of common differential
228 proteins in the six rats of the treated group on different days are shown in Table 2.

229 We analysed the differential proteins produced by D3 after e-cigarette smoking compared
230 with D0 (self-controls) in six treated rats. We found that two differential proteins were
231 commonly identified in six treated rats, and 16 differential proteins were commonly identified in
232 five experimental rats. After comparing the differential proteins produced by the control group
233 before and after with itself, the repeated proteins were screened out, resulting in differential
234 proteins with specific commonalities in the treated group. The details are presented in Table S1.

235 We also analysed the consensus differential proteins produced by six rats in the
236 experimental group on D12 after e-cigarette smoking versus D0 (self-control). Nine differential
237 proteins were commonly identified in six treated rats, and 18 differential proteins were
238 commonly identified in five experimental rats. After comparison with the differential proteins
239 produced by a single rat in the control group before and after treatment, the repeated proteins
240 were screened out, resulting in differential proteins with specific commonalities in the treated
241 group. The details are presented in Table S2.

242 When D15 was compared with D0, 7 differential proteins were commonly identified in 6
243 treated rats, and 45 differential proteins were commonly identified in 5 experimental rats. After
244 comparing the differential proteins produced by the control group before and after, the repeated
245 proteins were screened out, resulting in differential proteins with specific commonalities in the
246 experimental group. The details are presented in Table S3.

247 Finally, we analysed six rats in the experimental group for differential proteins screened by
248 self-comparison between D17 and D0, of which 7 differential proteins were commonly identified
249 from 6 rats in the experimental group and 42 differential proteins were commonly identified
250 from 5 rats in the experimental group. After comparing the differential proteins produced by the
251 control group before and after, the repeated proteins were screened out, resulting in differential
252 proteins with specific commonalities in the experimental group (see Table S4 for details).
253 Among the results presented at different time points, we found some consistency in the effects
254 caused by e-cigarette smoking in rats.

255 3.2.3 Functional comparison analysis

256 To investigate the function of these differential proteins, we performed functional analysis
257 of biological pathways using the DAVID database on the differential proteins coselected from
258 five or more treated rats (see Table S5 for details). Thirty-two of these biological processes were
259 enriched by differential proteins at both time points. We also performed signalling pathway
260 analysis of differentially identified proteins coidentified in five or more treated rats (Table 3).
261 Two of these signalling pathways were coenriched at both time points. These were Legionellosis
262 and Ferroptosis. In addition, we also identified many enriched signalling pathways associated
263 with respiratory diseases, such as the apelin signalling pathway^[33]^[34], folate biosynthesis
264 pathway^[35], and arachidonic acid metabolism^[36]. Of note, we also found two signalling pathways
265 associated with chemical carcinogenesis, that is, chemical carcinogenesis-DNA adducts and
266 chemical carcinogenesis-reactive oxygen species. These findings reinforce the sensitivity of the
267 urine proteome.

268 Discussion

269 In this study, we constructed a rat e-cigarette model and collected urine samples before,
270 during, and after e-cigarette smoking in rats on days 0, 3, 12, 15, and 17 to explore e-cigarettes
271 from the perspective of urine proteomics. To exclude the influence of individual variance, the
272 experiment used a single rat (before and after) for a controlled analysis, while the control group
273 was set up to rule out differences caused by rat growth and development. From the results
274 presented by the Venn diagram (Fig 4) of the differential proteins screened from the 6 rats in the
275 experimental group on days 3, 12, 15, and 17 compared with themselves on day 0, we found that
276 most of the differential proteins were personalized, indicating that the effects caused by e-
277 cigarettes on rats had strong individualized variance.

278 We analysed six treated rats on D3 compared with D0; among the resulting differential
279 proteins, fetuin-B was identified in five rats, all of which showed a significant decreasing trend.
280 There were also significant differences in urine protein on D12 and D15. It has been shown that
281 fetuin-B is a biomarker of COPD^[37], reflecting the sensitivity of the urine proteome. Surprisingly,
282 we also observed odourant-binding proteins (OBPs), including OBP1F and OBP2A, in urine
283 protein with significant changes on D3, of which OBP1F is mainly expressed in the nasal glands
284 of rats^[38], and OBP2A is also mainly transcribed in the nose of humans and rats^[39]. This result
285 suggests that in rats, smoking odourants can actually leave traces in the urine proteome.
286 Currently, the physiological role of OBPs is not fully understood^[40], and perhaps the urine
287 proteome can play a role in exploring the specific mechanism of action of OBPs. Annexin A2 is
288 widely used as a marker for a variety of tumours^[41]. In addition, László ZI et al. showed that
289 neurocadherin is one of the most important cell adhesion molecules during brain development
290 and plays an important role in neuronal formation, neuronal proliferation, differentiation and
291 migration, axonal guidance, synaptogenesis and synaptic maintenance^[42].

292 We also compared D12 with D0 of six rats in the experimental group. Among the
293 differential proteins produced in all six treated rats, OBP2B also showed a more consistent
294 upregulation. Unlike OBP2A, OBP2B is mainly expressed in reproductive organs and is weakly
295 expressed in organs of the respiratory system, such as the nose and lung^[43]. In addition,
296 desmocollin 3 is an essential protein for cell adhesion and desmosome formation and may
297 enhance angiogenesis with metastasis in nasopharyngeal carcinoma and is considered a
298 biomarker for some cancers, such as non-small cell lung cancer^[44]. It has also been shown that
299 Annexin A5 may affect the occurrence and development of pathological phenomena, such as
300 tumour diseases, pulmonary fibrosis and lung injury. Annexin A5 may also be used as a
301 biomarker in the study of diseases, such as tumours and asthma, and may promote the occurrence
302 and development of laryngeal cancer and nasopharyngeal carcinoma^[45]. We also screened an
303 important cellular target of the nicotine metabolite cotinine, gelsolin, which may affect basic
304 tumour transformation and metastasis processes, such as migration and apoptosis, through
305 gelatine^[46]. Heat shock protein, on the other hand, is reported to be a major marker affected by
306 cigarette smoke and is involved in signalling pathways associated with the cell cycle, cell death
307 and inflammation^{[47]-[49]}.

308 Comparing D15 with D0, the common differential proteins produced by the six
309 experimental rats included α -2u globulin. Ponmanickam P et al. showed that α -2u globulin may
310 act as a carrier of hydrophobic odourants in the preputial gland, which plays an important role in
311 producing pheromone-communicating olfactory signals in rats. Therefore, α -2u globulin is likely
312 to be involved in the transmission of olfactory signals in rats^[50].

313 Compared with those on D0, most of the common differential proteins produced by the six

314 rats in the experimental group on D17 were similar to those produced on other days, and all time
315 points contained odourant-binding proteins and proteins associated with a variety of diseases
316 (Table 2).

317 We performed signalling pathway analysis of differentially expressed proteins coidentified
318 in five or more treated rats (Table 3) and focused on two signalling pathways coenriched by the
319 two time points: Legionellosis and Ferroptosis. Pneumonia caused by Legionnaires' disease may
320 cause damage to the body similar to the mechanism of the effects of smoking e-cigarettes on the
321 body. M. Yoshida et al. showed that smoking can induce ferroptosis in epithelial cells, and this
322 signalling pathway is involved in the pathogenesis of chronic obstructive pulmonary disease^[51].
323 In addition, we also found enrichment of many signalling pathways associated with respiratory
324 diseases, such as the apelin signalling pathway^{[33][34]}, folate biosynthesis pathway^[35], and
325 arachidonic acid metabolism^[36]. Apelin is an endogenous ligand for the G protein-coupled
326 receptor APJ^[33], and the apelin/APJ pathway is closely related to the development of respiratory
327 diseases. Targeting the apelin/APJ system may be an effective therapeutic approach for
328 respiratory diseases^[34]. A study by Staniszavska-Sachadyn A et al. showed that serum folate
329 concentrations were higher in smokers than in healthy controls, and it was postulated that folate
330 synthesis is associated with an increased risk of lung cancer^[35]. Because the 23 enriched
331 signalling pathways include multiple signalling pathways directly related to the immune system,
332 cardiomyopathy, and atherosclerosis, we speculated that smoking e-cigarettes may affect the
333 immune system and cardiovascular system of rats. For the two enriched signalling pathways to
334 be associated with chemical carcinogenesis, it may be possible to verify previous findings that e-
335 cigarette smoke contains carcinogenic chemicals^[52].

336

337 Conclusion

338 There were strong individual variance in the differential proteins produced by rats after
339 smoking e-cigarettes under the same conditions. Fetuin-B, a biomarker of COPD, and annexin
340 A2, which is recognized as a multiple tumour marker, were coidentified in five out of six treated
341 rats' self-control samples on D3. Odourant-binding proteins expressed in the olfactory
342 epithelium were also identified in the urine proteome at multiple time points and were
343 significantly upregulated. How odourant-binding proteins expressed in the olfactory epithelium
344 end up in the urine after smoking e-cigarettes remains to be elucidated. Pathways enriched by the
345 differential proteins include the apelin signalling pathway, folate biosynthesis pathway,
346 arachidonic acid metabolism, chemical carcinogenesis-DNA adducts and chemical
347 carcinogenesis-reactive oxygen species. They have been reported to be associated with immune
348 system, cardiovascular system, respiratory system, etc. Urinary proteome could reflect the effects
349 of e-cigarettes in rats.

350

351

352

353 References

- 354 [1] Xinhuanet. Available online: [http://www.xinhuanet.com/politics/2019-11/06/c](http://www.xinhuanet.com/politics/2019-11/06/c1125199903.htm)
355 [1125199903.htm](http://www.xinhuanet.com/politics/2019-11/06/c1125199903.htm) (accessed on 6 November 2019).
356 [2] Bold KW, Kong G, Cavallo DA, Camenga DR, Krishnan-Sarin S. Reasons for trying E-
357 cigarettes and risk of continued use. *Pediatrics*. **2016**, 138(3):e20160895.

- 358 [3] Pipe AL, Mir H. E-Cigarettes Reexamined: Product Toxicity. *Can J Cardiol.* **2022**,
359 38(9),1395-1405.
- 360 [4] Cheng KA, Nichols H, McAdams HP, Henry TS, Washington L. Imaging of Smoking
361 and Vaping Related Diffuse Lung Injury. *Radiol Clin North Am.* **2022**, 60(6):941-950.
- 362 [5] Fetterman JL, Keith RJ, Palmisano JN, McGlasson KL, Weisbrod RM, Majid S, Bastin
363 R, Stathos MM, Stokes AC, Robertson RM, Bhatnagar A, Hamburg NM. Alterations in vascular
364 function associated with the use of combustible and electronic cigarettes. *J Am Heart Assoc.*
365 **2020**, 9(9): e014570
- 366 [6] Lee WH, Ong SG, Zhou Y, Tian L, Bae HR, Baker N, Whitlatch A, Mohammadi L, Guo
367 H, Nadeau KC, Springer ML, Schick SF, Bhatnagar A, Wu JC. Modeling cardiovascular risks of
368 e-cigarettes with human-induced pluripotent stem cell-derived endothelial cells. *J Am Coll*
369 *Cardiol.* **2019**, 73(21): 2722-2737.
- 370 [7] Espinoza-Derout J, Shao XM, Bankole E, Hasan KM, Mtume N, Liu Y, Sinha-Hikim AP,
371 Friedman TC. Hepatic DNA damage induced by electronic cigarette exposure is associated with
372 the modulation of NAD⁺/PARP1/SIRT1 axis. *Front Endocrinol (Lausanne).* **2019**, 10: 320.
- 373 [8] Lee HW, Park SH, Weng MW, Wang HT, Huang WC, Lepor H, Wu XR, Chen LC, Tang
374 MS. E-cigarette smoke damages DNA and reduces repair activity in mouse lung, heart, and
375 bladder as well as in human lung and bladder cells. *Proc Natl Acad Sci USA.* **2018**, 115(7):
376 E1560-E1569.
- 377 [9] Martin EM, Clapp PW, Rebuli ME, Pawlak EA, Glista-Baker E, Benowitz NL, Fry RC,
378 Jaspers I. E-cigarette use results in suppression of immune and inflammatory-response genes in
379 nasal epithelial cells similar to cigarette smoke. *Am J Physiol Lung Cell Mol Physiol.* **2016**,
380 311(1): L135-L144.
- 381 [10] Ballbè M, Fu M, Masana G, Pérez-Ortuño R, Gual A, Gil F, Olmedo P, García-Algar Ó,
382 Pascual JA, Fernández E. Passive exposure to electronic cigarette aerosol in pregnancy: A case
383 study of a family. *Environ Res.* **2022**, 8:114490.
- 384 [11] Aslaner DM, Alghothani O, Saldana TA, Ezell KG, Yallourakis MD, MacKenzie DM,
385 Miller RA, Wold LE, Gorr MW. E-cigarette vapor exposure in utero causes long-term
386 pulmonary effects in offspring. *Am J Physiol Lung Cell Mol Physiol.* **2022** Oct 11. doi:
387 10.1152/ajplung.00233.2022. Epub ahead of print. PMID: 36218276.
- 388 [12] Ballbè M, Martínez-Sánchez JM, Sureda X, Fu M, Pérez-Ortuño R, Pascual JA, Saltó E,
389 Fernández E. Cigarettes vs. e-cigarettes: Passive exposure at home measured by means of
390 airborne marker and biomarkers. *Environ Res.* **2014**, 135:76-80.
- 391 [13] Kyle Strimbu, Jorge A Tavel. What are biomarkers? *Current Opinion in HIV and AIDS.*
392 **2010**, 5(6).
- 393 [14] Gerszten Robert E, Wang Thomas J. The search for new cardiovascular biomarkers.
394 *Nature.* **2008**, 451(7181).
- 395 [15] Gao, Y. Urine-an untapped goldmine for biomarker discovery? *Science China. Life*
396 *sciences*, **2013**. 56(12): p. 1145-1146.
- 397 [16] Wu J, Li X, Zhao M, Huang H, Sun W, Gao Y. Early Detection of Urinary Proteome
398 Biomarkers for Effective Early Treatment of Pulmonary Fibrosis in a Rat Model. *Proteomics*
399 *Clin Appl.* **2017**, 11(11-12).
- 400 [17] Qin W, Li L, Wang T, Huang H, Gao Y. Urine Proteome Changes in a TNBS-Induced
401 Colitis Rat Model. *Proteomics Clin Appl.* **2019**, 13(5):e1800100.
- 402 [18] Wu J, Zhang J, Wei J, Zhao Y, Gao Y. Urinary biomarker discovery in gliomas using
403 mass spectrometry-based clinical proteomics. *Chin Neurosurg J.* **2020**, 6:11.
- 404 [19] Hao Y, Reyes LT, Morris R, Xu Y, Wang Y, Cheng F. Changes of protein levels in
405 human urine reflect the dysregulation of signaling pathways of chronic kidney disease and its
406 complications. *Sci Rep.* **2020**, 10(1):20743.

- 407 [20] Ni M, Zhou J, Zhu Z, Yuan J, Gong W, Zhu J, Zheng Z, Zhao H. A Novel Classifier
408 Based on Urinary Proteomics for Distinguishing Between Benign and Malignant Ovarian
409 Tumors. *Front Cell Dev Biol.* **2021**, 9:712196.
- 410 [21] Davies JC, Carlsson E, Midgley A, Smith EMD, Bruce IN, Beresford MW, Hedrich CM;
411 BILAG-BR and MRC MASTERPLANS Consortia. A panel of urinary proteins predicts active
412 lupus nephritis and response to rituximab treatment. *Rheumatology (Oxford).* **2021**, 60(8):3747-
413 3759.
- 414 [22] Meng W, Xu D, Meng Y, Zhang W, Xue Y, Zhen Z, Gao Y. Changes in the urinary
415 proteome in rats with regular swimming exercise. *Peer J.* **2021**, 9:e12406
- 416 [23] Virreira Winter S, Karayel O, Strauss MT, Padmanabhan S, Surface M, Merchant K,
417 Alcalay RN, Mann M. Urinary proteome profiling for stratifying patients with familial
418 Parkinson's disease. *EMBO Mol Med.* **2021**, 13(3):e13257.
- 419 [24] Seol W, Kim H, Son I. Urinary Biomarkers for Neurodegenerative Diseases. *Exp*
420 *Neurobiol.* **2020**, 29(5):325-333.
- 421 [25] Watanabe Y, Hirao Y, Kasuga K, Tokutake T, Kitamura K, Niida S, Ikeuchi T,
422 Nakamura K, Yamamoto T. Urinary Apolipoprotein C3 Is a Potential Biomarker for Alzheimer's
423 Disease. *Dement Geriatr Cogn Dis Extra.* **2020**, 10(3): p. 94-104.
- 424 [26] Huan Y, Wei J, Zhou J, Liu M, Yang J, Gao Y. Label-Free Liquid Chromatography-Mass
425 Spectrometry Proteomic Analysis of the Urinary Proteome for Measuring the Escitalopram
426 Treatment Response From Major Depressive Disorder. *Front Psychiatry.* **2021**, 12:700149.
- 427 [27] Meng W, Huan Y, Gao Y. Urinary proteome profiling for children with autism using
428 data-independent acquisition proteomics. *Transl Pediatr.* **2021**, 10(7):1765-1778.
- 429 [28] Yuqing Liu, Ziyun Shen, Chenyang Zhao, Youhe Gao. Urine. Proteomic analysis of the rat
430 e-cigarette model. *bioRxiv.* **2022**.11.19.517186; doi: <https://doi.org/10.1101/2022.11.19.517186>.
- 431 [29] Wisniewski, J. R., Zougman, A., Nagaraj, N. & Mann, M. Universal sample preparation
432 method for proteome analysis. *Nat Methods.* **2009**, 6: 359–362.
- 433 [30] Wu, J., Guo, Z. & Gao, Y. Dynamic changes of urine proteome in a Walker 256 tumor-
434 bearing rat model. *Cancer Med.* **2017**, 6: 2713–2722.
- 435 [31] Wei J, Ni N, Meng W, Gao Y. Early urine proteome changes in the Walker-256 tail-vein
436 injection rat model. *Sci Rep.* **2019**, 9: 13804.
- 437 [32] Nature Protocols **2009**, 4(1):44 & Nucleic Acids Res. **2009**, 37(1):1
- 438 [33] Tatemoto K, Hosoya M, Habata Y, Fujii R, Kakegawa T, Zou MX, Kawamata Y,
439 Fukusumi S, Hinuma S, Kitada C, Kurokawa T, Onda H, Fujino M. Isolation and
440 characterization of a novel endogenous peptide ligand for the human APJ receptor. *Biochem*
441 *Biophys Res Commun.* **1998**, 251(2):471-476.
- 442 [34] Yan J, Wang A, Cao J, Chen L. Apelin/APJ system: an emerging therapeutic target for
443 respiratory diseases. *Cell Mol Life Sci.* **2020**, 77(15):2919-2930.
- 444 [35] Stanisławska-Sachadyn A, Borzyszkowska J, Krzemiński M, Janowicz A, Dziadziuszko
445 R, Jassem J, Rzyman W, Limon J. Folate/homocysteine metabolism and lung cancer risk among
446 smokers. *PLoS ONE.* **2019**, 14:e0214462.
- 447 [36] Giudetti AM, Cagnazzo R. Beneficial effects of n-3 PUFA on chronic airway
448 inflammatory diseases. *Prostaglandins Other Lipid Mediat.* **2012**, 99(3-4):57-67.
- 449 [37] Diao WQ, Shen N, Du YP, Liu BB, Sun XY, Xu M, He B. Fetuin-B (FETUB): a Plasma
450 Biomarker Candidate Related to the Severity of Lung Function in COPD. *Sci Rep.* **2016**,
451 6:30045.
- 452 [38] Aragona P, Puzzolo D, Micali A, Ferreri G, Britti D. Morphological and morphometric
453 analysis on the rabbit conjunctival goblet cells in different hormonal conditions. *Exp Eye Res.*
454 **1988**, 66:81-88

- 455 [39] Briand L, Eloit C, Nespoulous C, Bézirard V, Huet JC, Henry C, Blon F, Trotier D,
456 Pernollet JC. Evidence of an odorant-binding protein in the human olfactory mucus: location,
457 structural characterization, and odorant-binding properties. *Biochemistry*. **2002**, 41(23):7241-
458 7252
- 459 [40] Redl B, Habeler M. The diversity of lipocalin receptors. *Biochimie*. **2022**, 192:22-29.
- 460 [41] Huang Y, Jia M, Yang X, Han H, Hou G, Bi L, Yang Y, Zhang R, Zhao X, Peng C,
461 Ouyang X. Annexin A2: The diversity of pathological effects in tumorigenesis and immune
462 response. *Int J Cancer*. **2022**, 151(4):497-509.
- 463 [42] László ZI, Lele Z. Flying under the radar: CDH2 (N-cadherin), an important hub
464 molecule in neurodevelopmental and neurodegenerative diseases. *Front Neurosci*. **2022**,
465 16:972059.
- 466 [43] Lacazette E, Gachon AM, Pitiot G. A novel human odorant-binding protein gene family
467 resulting from genomic duplicons at 9q34: differential expression in the oral and genital spheres.
468 *Hum Mol Genet*. **2000**, 9(2):289-301.
- 469 [44] Ezzat Nel-S, Tahoun N. The role of Napsin-A and Desmocollin-3 in classifying poorly
470 differentiating non-small cell lung carcinoma. *J Egypt Natl Canc Inst*. **2016**, 28(1):13-22.
- 471 [45] Xi Zhang, QingYu Meng, Jian Jing . Human Annexin A5: from Biomarkers to
472 Therapeutic Candidates. *Chinese Journal of Biochemistry and Molecular Biol*. **2022**, 38(10):
473 1311-1321.
- 474 [46] Nowak JM, Klimaszewska-Wiśniewska A, Izdebska M, Gagat M, Grzanka A. Gelsolin is
475 a potential cellular target for cotinine to regulate the migration and apoptosis of A549 and T24
476 cancer cells. *Tissue Cell*. **2015**, 47(1):105-14.
- 477 [47] Gál K, Cseh A, Szalay B, Rusai K, Vannay A, Lukácsovits J, Heemann U, Szabó AJ,
478 Losonczy G, Tamási L, Müller V. Effect of cigarette smoke and dexamethasone on Hsp72
479 system of alveolar epithelial cells. *Cell Stress Chaperones*. **2011**, 16:369-378.
- 480 [48] Hulina-Tomašković A, Heijink IH, Jonker MR, Somborac-Baćura A, Grdić Rajković M,
481 Rumora L. Pro-inflammatory effects of extracellular Hsp70 and cigarette smoke in primary
482 airway epithelial cells from COPD patients. *Biochimie*. **2019**, 156:47-58.
- 483 [49] M.H. Parseghian, S.T. Hobson, R.A. Richieri. Targeted heat shock protein 72 (HSP72)
484 for pulmonary cytoprotection. *Ann. N. Y. Acad. Sci*. **2016**, 1374:78.
- 485 [50] Ponmanickam P, Archunan G. Identification of alpha-2u globulin in the rat preputial
486 gland by MALDI-TOF analysis. *Indian J Biochem Biophys*. **2006**, 43(5):319-22.
- 487 [51] Yoshida M, Minagawa S, Araya J, Sakamoto T, Hara H, Tsubouchi K, Hosaka Y,
488 Ichikawa A, Saito N, Kadota T, Sato N, Kurita Y, Kobayashi K, Ito S, Utsumi H, Wakui H,
489 Numata T, Kaneko Y, Mori S, Asano H, Yamashita M, Odaka M, Morikawa T, Nakayama K,
490 Iwamoto T, Imai H, Kuwano K. Involvement of cigarette smoke-induced epithelial cell
491 ferroptosis in COPD pathogenesis. *Nat. Commun*. **2019**, 10:1-14.
- 492 [52] Eshraghian EA, Al-Delaimy WK. A review of constituents identified in e-cigarette
493 liquids and aerosols. *Tob Prev Cessat*. **2021**, 10;7:10.

Table 1 (on next page)

Changes in differential protein expression during e-cigarette smoking in individual rats.

1 **Table 1. Changes in differential protein expression during e-cigarette smoking in individual rats.**

Days	Differential protein expression	Control group(pcs)					Treated group(pcs)					
		Rat	Rat	Rat	Rat	Rat	Rat	Rat	Rat	Rat	Rat	Rat
		1	2	3	4	5	1	2	3	4	5	6
	Total	215	208	208	162	96	181	203	177	331	144	490
Day3/Day0	↑	89	83	82	71	59	51	87	58	127	60	199
	↓	126	125	126	91	37	130	116	119	204	84	291
	Total	401	257	214	275	217	260	265	188	336	173	533
Day12/Day0	↑	175	115	82	126	106	117	112	80	152	93	241
	↓	226	142	132	149	111	143	153	108	184	80	292
	Total	288	255	337	289	505	350	341	261	402	246	512
Day15/Day0	↑	124	141	130	104	312	125	153	104	163	151	214
	↓	173	114	207	185	193	225	188	157	239	95	298
	Total	395	264	289	320	191	266	283	199	290	475	518
Day17/Day0	↑	183	134	111	157	142	117	140	81	124	312	251
	↓	212	130	178	163	49	149	143	188	166	163	267
	Total	395	264	289	320	191	266	283	199	290	475	518

2

Table 2 (on next page)

Trends of common differential proteins in 6 rats in the experimental group on different days.

1 **Table 2. Trends of common differential proteins in 6 rats in the experimental group on different days.**

UniProt accession	Human ortholog	Protein name	Rat amount(pcs) and trend				Related to OBP	Related to human disease
			D3	D12	D15	D17		
G3V803	P19022	Cadherin-2, Neural cadherin	5↓	6↓	5↓	5↓	-	[42]
P14668	P08758	Annexin A5	-	5↑	5↑	5↑ 1↓	-	[45]
Q99041	P49221	Protein-glutamine gamma-glutamyltransferase 4	-	1↑ 4↓	3↑ 2↓	2↑ 4↓	-	-
P20761	-	Ig gamma-2B chain C region	-	4↑ 1↓	5↑	4↑ 1↓	-	-
B3EY84	Q9NY56	Lipocalin 13, Odorant-binding protein 2A	5↓	-	5↑ 1↓	5↑	[39]	-
P07151	P61769	Beta-2-microglobulin	4↑ 1↓	4↑ 1↓	6↑	-	-	-
Q6IRS6	Q9UGM5	Fetuin-B	5↓	6↓	6↓	-	-	[37]
P27590	P07911	Uromodulin	-	-	5↑	5↑	-	-
Q9JJH9	-	Alpha-2u globulin	-	-	5↑	5↑	[50]	-
P0DMW0	P0DMV8	Heat shock 70 kDa protein 1A	-	4↑ 1↓	-	3↑ 2↓	-	[47-49]
M0RDH1	-	Odorant-binding protein 2B	-	5↑ 1↓	-	5↑	[43]	-
Q68FP1	P06396	Gelsolin	-	5↑	-	5↑ 1↓	-	[46]
A0A0G2K230	Q14574	Desmocollin 3	-	5↑	-	5↑	-	[44]
P51635	P14550	Aldo-keto reductase family 1 member A1	-	5↑	-	4↑ 1↓	-	-
Q64724	-	C-CAM4	5↓	-	-	1↑ 4↓	-	-
P05545	-	Serine protease inhibitor A3K	5↓	-	-	5↓	-	-
Q07936	P07355	Annexin A2	4↑ 1↓	-	-	2↑ 3↓	-	[41]
D4A9V5	-	Lysyl oxidase homolog	-	6↓	5↓	-	-	-
P46413	P48637	Glutathione synthetase	5↓	-	5↓	-	-	-
D4AE68	-	Guanine nucleotide-binding protein G(q) subunit alpha	3↑ 2↓	5↑ 1↓	-	-	-	-
Q9QYU9	-	odorant-binding protein 1F	5↓	-	-	-	[38]	-
Q9JJI3	-	Alpha-2u globulin	-	-	6↑	-	[50]	-

2

Table 3 (on next page)

Signal pathways enriched in common differential proteins produced during e-cigarette smoking in five or more treated rats.

1 **Table 3. Signal pathways enriched in common differential proteins produced during e-cigarette smoking in five or more**
 2 **treated rats.**

Pathway	P-value				Related to human disease
	D3	D12	D15	D17	
GnRH secretion	4.20E-02	-	-	-	-
Apelin signaling pathway	8.80E-02	-	-	-	[33-34]
Antigen processing and presentation	-	4.00E-03	-	-	-
Oestrogen signaling pathway	-	9.40E-03	-	-	-
Human immunodeficiency virus 1 infection	-	2.70E-02	-	-	-
Legionellosis	-	6.30E-02	-	9.30E-02	-
Longevity regulating pathway - multiple species	-	6.90E-02	-	-	-
Renin secretion	-	7.80E-02	-	-	-
Arrhythmogenic right ventricular cardiomyopathy	-	8.30E-02	-	-	-
Folate biosynthesis	-	-	1.10E-03	-	[35]
Metabolism of xenobiotics by cytochrome P450	-	-	6.90E-03	-	-
Chemical carcinogenesis - DNA adducts	-	-	6.90E-03	-	-
Arachidonic acid metabolism	-	-	8.00E-03	-	[36]
Metabolic pathways	-	-	3.80E-02	-	-
Chemical carcinogenesis - reactive oxygen species	-	-	5.70E-02	-	-
Ferroptosis	-	-	6.80E-02	6.80E-02	[51]
Mineral absorption	-	-	-	4.00E-03	-
Glycolysis/Gluconeogenesis	-	-	-	5.60E-03	-
Phenylalanine metabolism	-	-	-	3.00E-02	-
Histidine metabolism	-	-	-	4.10E-02	-
Lipid and atherosclerosis	-	-	-	4.70E-02	-
beta-Alanine metabolism	-	-	-	5.10E-02	-
Tyrosine metabolism	-	-	-	6.20E-02	-

3

Figure 1

Workflow for urine proteomic analysis in rat e-cigarette models.

In the experimental group, urine samples were collected before and on days 3, 6, 9, and 12 after smoking e-cigarettes and on days 1 and 3 after stopping smoking e-cigarettes. After urine samples were collected and processed in the experimental and control groups, the protein groups of the two groups were identified using liquid chromatography coupled with tandem mass spectrometry (LC-MS/MS) to quantitatively analyze the damage caused to the rat body at different stages of smoking e-cigarettes.

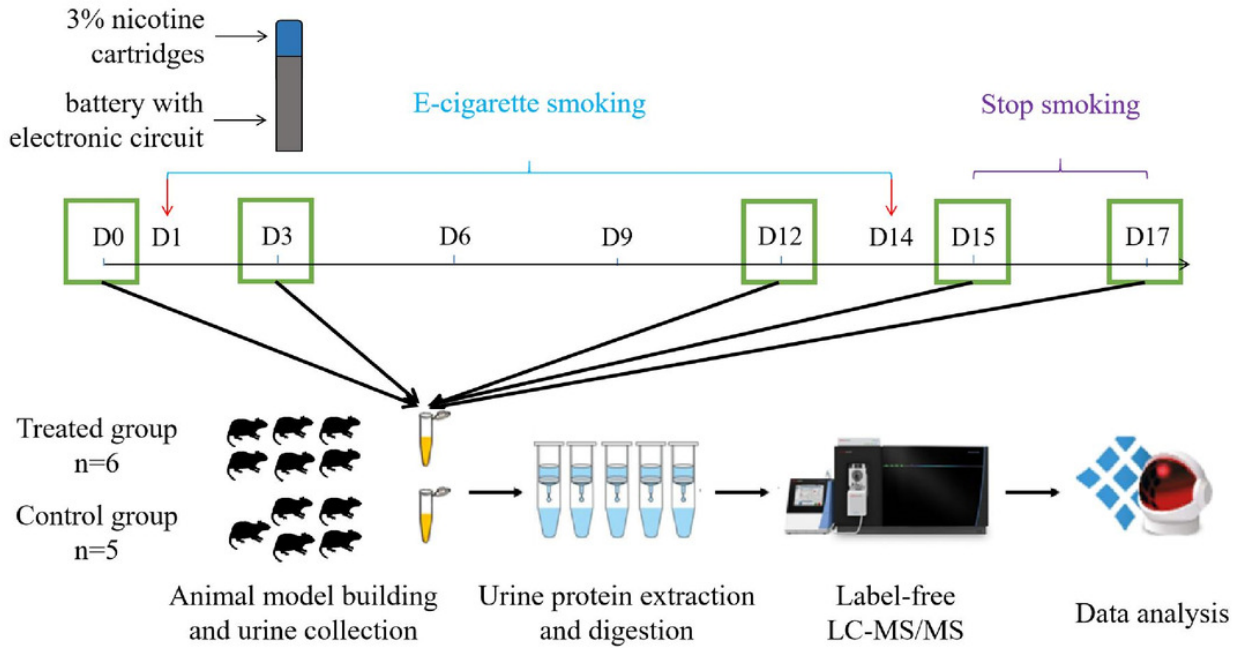


Figure 2

Body weight changes in the rat e-cigarette model.

The obtained results are shown as the means \pm SDs for the control group (n=5) and the treated group (n=6).

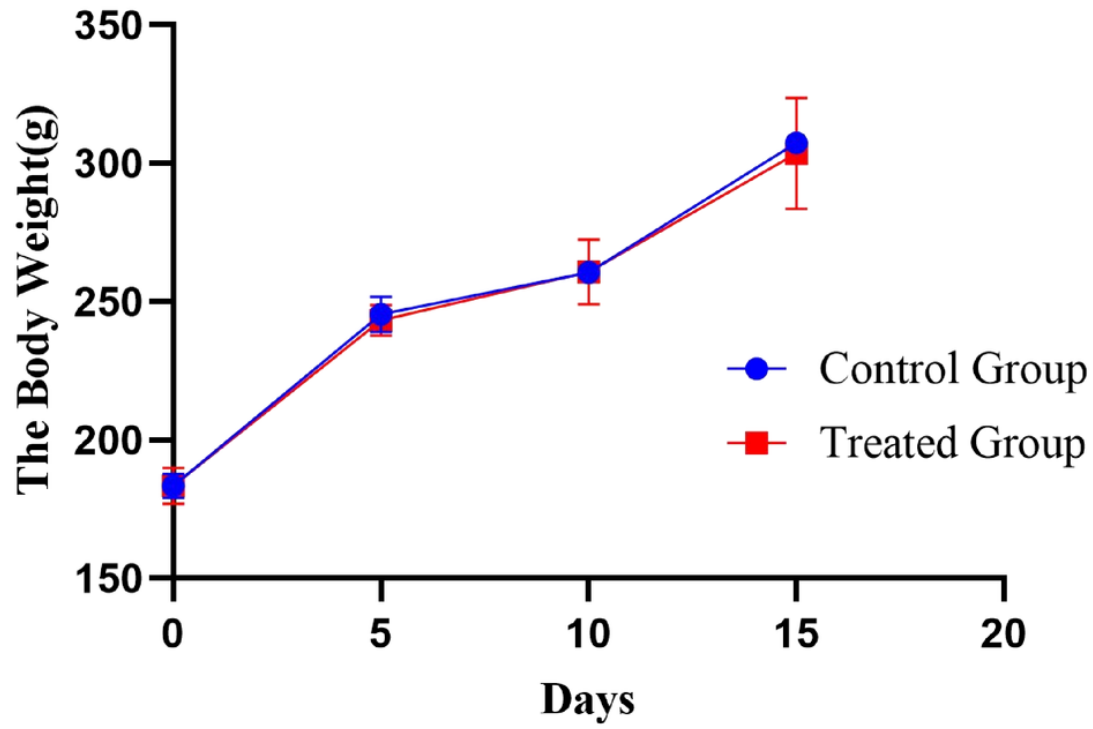


Figure 3

Volcano plots of differential proteins produced by six experimental rats at different time points vs. Day0.

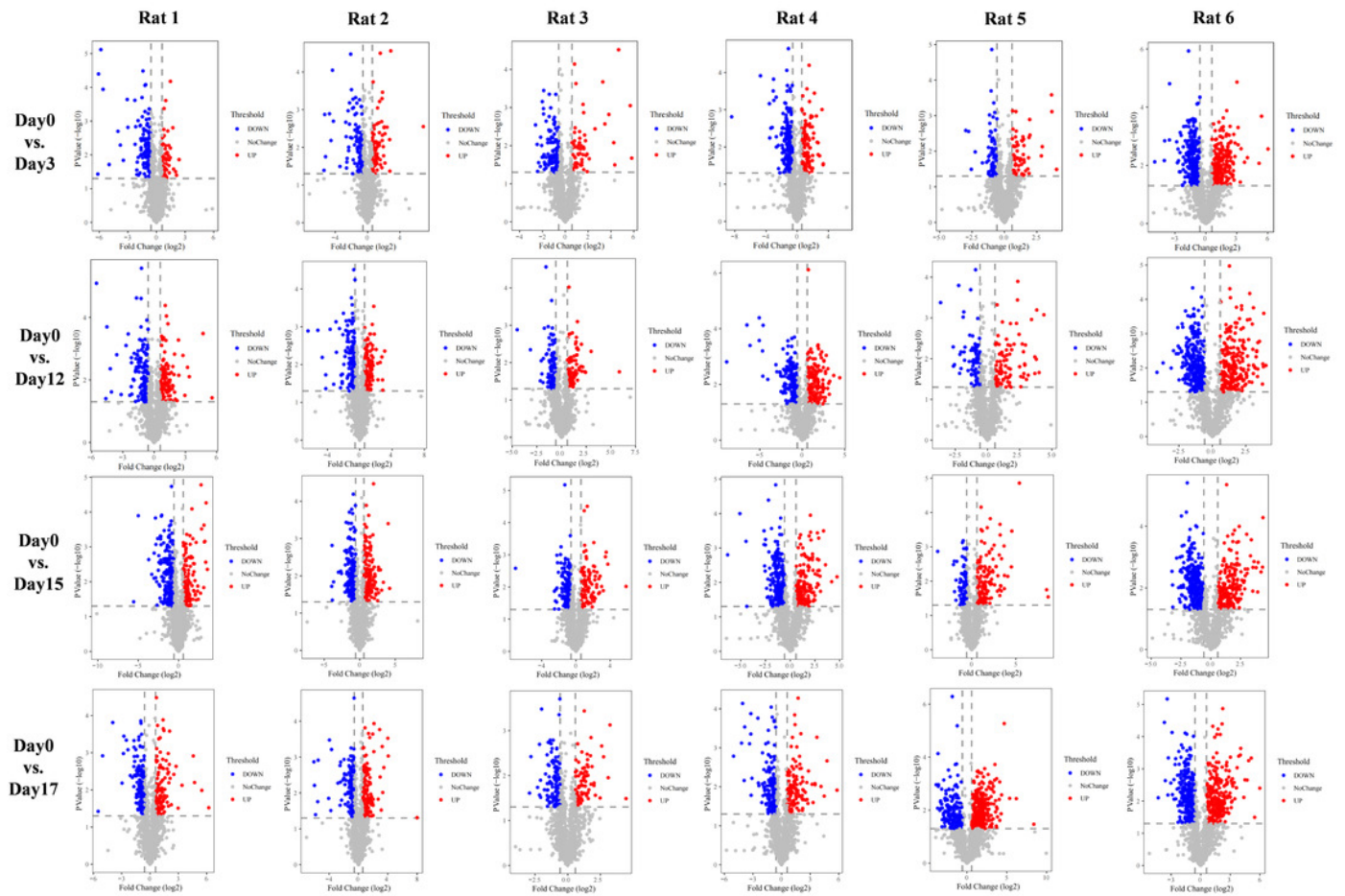


Figure 4

Differential proteins Venn diagram produced by 6 treated rats and their own control.

(A) D3 vs. D0. (B) D12 vs. D0. (C) D15 vs. D0. (D) D17 vs. D0.

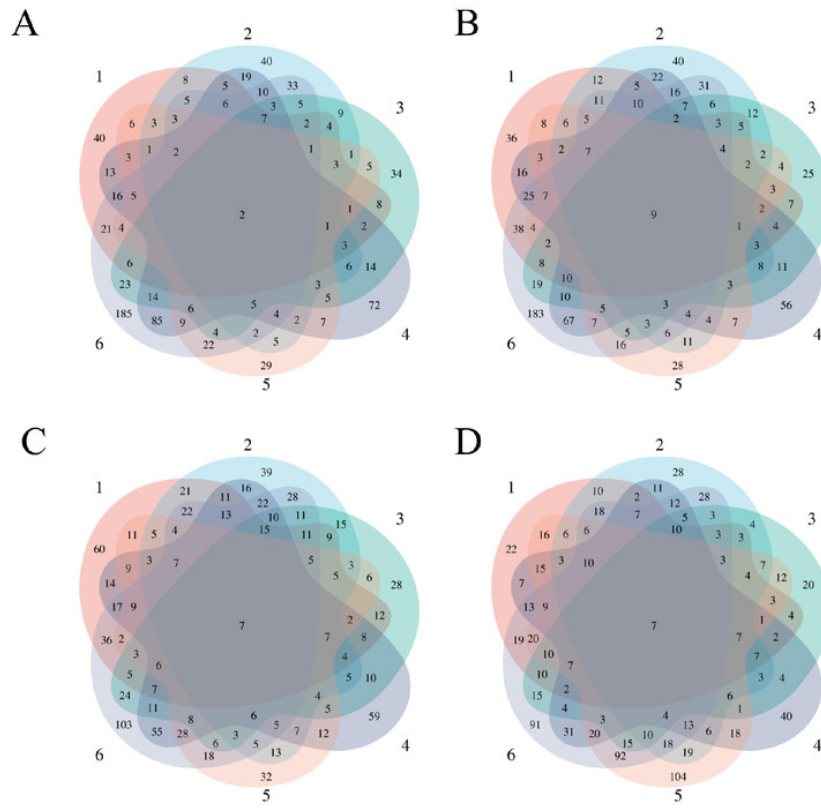


Figure 5

Venn diagram of common differential proteins in 6 rats in the experimental group on different days.

